Available online at www.sciencedirect.com

ScienceDirect

Defence Technology 12 (2016) 464–472

www.elsevier.com/locate/dt

A comparative evaluation of microstructural and mechanical behavior of fiber laser beam and tungsten inert gas dissimilar ultra high strength steel welds

Jaiteerth R. JOSHI [a], Mastanaiah POTTA [a,*], Kumar ADEPU [b], Ramesh Kumar KATTA [a], Madhusudhan Reddy GANKIDI [c]

[a] *Defence Research and Development Laboratory, Kanchanbagh, Hyderabad, Telangana 500058, India*
[b] *National Institute of Technology, Warangal, Telangana 502205, India*
[c] *Defence Metallurgical Research Laboratory, Kanchanbagh, Hyderabad, Telangana 500058, India*

Received 13 July 2016; revised 6 August 2016; accepted 8 August 2016

Available online 8 September 2016

Abstract

The influence of different welding processes on the mechanical properties and the corresponding variation in the microstructural features have been investigated for the dissimilar weldments of 18% Ni maraging steel 250 and AISI 4130 steel. The weld joints are realized through two different fusion welding processes, tungsten inert arc welding (TIG) and laser beam welding (LBW), in this study. The dissimilar steel welds were characterized through optical microstructures, microhardness survey across the weldment and evaluation of tensile properties. The fiber laser beam welds have demonstrated superior mechanical properties and reduced heat affected zone as compared to the TIG weldments.

Keywords: TIG welding; Fiber laser; AISI 4130 steel; Laser beam welding; Maraging steel

1. Introduction

18% Ni maraging steels are extensively used in aerospace and defense applications because of their incomparable fracture toughness coupled with high tensile strength. The steels achieve superior mechanical properties through a simple low temperature precipitation hardening heat treatment and they are easily weldable as well [1]. Whereas one of the chromium-molybdenum steels, AISI 4130 steel, possesses moderate strength and reasonable ductility in hardened and tempered condition. This feature of AISI 4130 steel makes it highly suitable for various critical applications in air craft and automobile industries [2]. In many cases combination of steels in structures is necessary for technical and economical reasons. Therefore dissimilar joints are inevitable for connecting the components/systems made of different materials. Welding is a major route adopted for fabrication of such components. Though enough number of articles are noticed in open literature about fusion welding of either of these steels in their similar combinations, very few articles are published about dissimilar welding of these two ultra high strength steels. The high strength low alloys (like AISI 4130 steel) are found to be very sensitive to the heat affected zone softening behavior as compared to that of maraging steels [3,4]. So performance of weld joint majorly depends on this softer HAZ region (which is a weak link in the entire weldment) and thus controlling the extent of softening is highly essential in real time applications in order to realize better performing structures or pressure vessels.

Nascimento and Voorwald [5] have studied the repair welding effects on the fatigue strength of aerospace structure made of AISI 4130 steel. They reported that during cyclic loading, the failure of AISI 4130 steel weld joint has occurred in the HAZ region due to the presence of tempered martensite that was formed during repair welding process. There exist several ways to control the HAZ softening behavior during welding of high strength low alloy steels. One way of controlling the degree of softening is by means of applying external cooling methods during and after welding process so that the excess welding heat input can be extracted effectively from the HAZ region. Yan et al. [6] have imposed faster cooling rates in HAZ region of high strength offshore steel by employing

Peer review under responsibility of China Ordnance Society.
* Corresponding author. Tel.: +914024583528.
E-mail address: mastanaiah_p@rediffmail.com (M. POTTA).

http://dx.doi.org/10.1016/j.dt.2016.08.003

compressed air immediately after submerged arc welding process. They found that the fast cooling has improved the efficiency and low temperature impact toughness of the offshore steel weld joints by reducing the width of HAZ. Dong et al. [7] have reported that reducing the welding heat input during gas tungsten arc welding of HSLA steel has substantially increased the hardness and thus the strength of HAZ region by limiting the formation of martensite.

Joshi et al. [8] have reported effect of different welding techniques and external heat extraction methods on heat affected zone softening in dissimilar metal weld joints of maraging steel and AISI 4130 steel. They used continuous current and pulsed current modes in TIG and applied an external water re-circulating copper jacket to extract the excess welding heat input from HAZ region. In their study, Joshi et al. [8] have reported that use of pulsed TIG welding process along with external cooling method has drastically reduced HAZ softening and has resulted in dissimilar steel welds with superior mechanical properties.

The other way of reducing the heat affected zone softening is by employing low heat input welding processes such as electron beam welding or laser beam welding processes in place of conventional arc based fusion welding processes. Huang et al. [9] have studied the influence of post weld heat treatments on the strength and resulting residual stresses in electron beam welded joints of AISI 4130 steel. Their work has shown that subjecting weld joints to heat treatment results in reduced residual stresses and improved the percentage elongation. The work by Chang and Wang [10] has demonstrated that by applying electron beam and furnace post weld treatments on AISI 4130 steel EB welds, it is possible to change the nature of tensile residual stresses into compressive stresses. This reversal of mode of residual stresses has drastically improved the resistance offered by EB welds to fatigue crack growth. Souza Neto et al. [11] have compared the mechanical properties of TIG and laser beam weld joints of AISI 4130 steel. Their study revealed that HAZ width of laser beam welds of AISI 4130 steel are ten times lesser than that of gas tungsten arc welds.

In the recent past, fiber lasers are invented and introduced into manufacturing sector. The fiber lasers score better than conventional CO_2 type lasers in terms of high energy density, deeper, narrower and possible high welding speeds especially in thin walled cross sections [12]. These high aspect ratio welds are produced with a relatively low heat input. As a consequence fiber laser welding can be used to a particular advantage where it is desirable to minimize HAZ softening, distortion and shrinkage stresses. Though the work by Joshi et al. [8] has revealed the possible improvement of the mechanical properties of dissimilar steel TIG weld joints of maraging steel and AISI 4130 steel, still the joint efficiency in terms of yield strength was reported as 72%. There exists further scope to improve the joint efficiency beyond 72%. In a quest to perceive the maximum possible joint efficiency for this dissimilar steel welds, advanced fiber laser beam welding process was employed and studied in this work. Though it is a well established fact that the laser beam welds impose less heat input compared to those of TIG welds, interaction of laser beam particularly on joining of dissimilar steels cited above is not reported.

However, very few articles are reported on the application of laser beam welding process in joining the high strength steels. The studies on dissimilar fusion welding of maraging steel and AISI 4130 steel are very scarcely available in open literature. The goal of current work is to bring out a comprehensive understanding about the mechanical and microstructural characteristics of dissimilar steel welds of maraging steel and AISI 4130 steel produced by tungsten inert welding and laser beam welding processes. This investigation assumes to be important as there exists a scarce literature on the subject, in particular, on dissimilar welding of the two ultra high strength steels under consideration.

2. Experimental procedure

2.1. Parent materials

The parent materials considered for investigation are AISI 4130 steel and 18% Ni maraging steel of MDN-250 variety. The maraging steel was taken in the form of a thin walled flow formed test ring with an external diameter of 225 mm, thickness of 2 mm and 125 mm of length. The test ring was subjected to a low temperature aging heat treatment: 485 °C/ soaking for 3.5 hours and followed by air cool. A test ring of similar dimensions made of AISI 4130 steel was machined from a forging which undergone a heat treatment of hardening (870 °C/1 hour/oil quench) followed by tempering (260 °C/1 hour/air cool). The chemical composition and tensile properties of both the parent materials are mentioned in Table 1.

2.2. Welding trials

The test rings of maraging steel and AISI 4130 steel were TIG welded in a single pass by both in continuous current and pulsed welding modes using a W_2 grade maraging steel filler wire of diameter 1.6 mm. The filler wire of maraging steel was primarily employed because of its superior as-deposited strength and weldability as compared to that of AISI 4130 steel [1]. The chemical composition of W_2 grade maraging steel filler wire is mentioned in Table 2 and the TIG welding parameters are given in Table 3.

Another set of test rings were welded using a CNC solid state laser beam welding machine built by M/s. Arnold, Germany. Laser beam welding trial was conducted without

Table 1
Chemical composition(wt%) and tensile properties of parent materials.

	C	Ni	Cr	Co	Mo	Ti	Al	Mn	Si	Fe	UTS/MPa	0.2%YS MPa	%El./
Maraging steel	0.02	18.9	–	8.1	4.9	0.4	0.15	0.04	–	Bal.	1839	1810	2.9
AISI 4130 steel	0.3	–	0.86	–	0.25	–	–	0.48	0.26	Bal.	1530	1215	8.5

Table 2
Chemical composition of W_2 grade maraging steel filler wire.

Ni	C	Al	Co	Ti	Mo	Fe
18.2	0.006	0.46	11.9	0.16	2.5	Remainder

Table 3
Parameters of different welding processes employed.

Welding condition	Parameters
Continuous current – TIG	Welding current = 65 Amp, Arc voltage = 10 Volts and Travel speed = 64 mm/min
Pulsed current – TIG	Peak current: I_p = 90 Amp, Back ground current: I_b = 25 Amp, % Pulse on time =50%,Pulse frequency = 4 HZ, Arc voltage = 10 Volts, Travel speed = 64 mm/min
Laser beam welding	Type of laser: Fiber, Laser beam power: 3700 W, Welding speed = 2000 mm/min. Focal length of welding head = 300 mm, Dia of optical fiber = 100 μm.

addition of any filler wire with square butt edge preparation. The Laser beam welding parameters are mentioned in Table 3. In order to maintain an analogous heat flow conditions, the dimensions and welding fixture set up were maintained the same during all the welding experimentations. Typical weld fixturing setup for both TIG and Laser beam welding processes is shown in Fig. 1.

2.3. Measurement of temperatures in HAZ of AISI 4130 steel

The HAZ of AISI 4130 steel is determined to undergo softening phenomenon due to exposure to the welding heat input. In order to measure the peak temperatures experienced by this HAZ during welding, k-type thermocouples were employed in combination with a GRAPHTECH make data logger (model No: GL900). The temperatures were recorded at a rate of 50 readings per second. The reported temperatures in this work are an average of three temperature readings.

2.4. Testing of weld joints

The dissimilar steel welds joints were examined through the non-destructive tests such as X-ray radiography and dye penetrant tests in order to reveal the presence of sub-surface and surface defects respectively. The transverse tensile test specimens were extracted from the defect free zones as per the drawing specified in the standard ASTM A 370. INSTRON make universal tensile testing machine was employed to evaluate the tensile properties i.e., ultimate tensile strength, 0.2% yield strength and percentage elongation. The dissimilar steel joint was subjected to microhardness survey across the weldment at mid thickness using MATSUZAWA make hardness tester with the application of 100 gf load and maintaining a spacing of 0.2 mm between any two indentations.

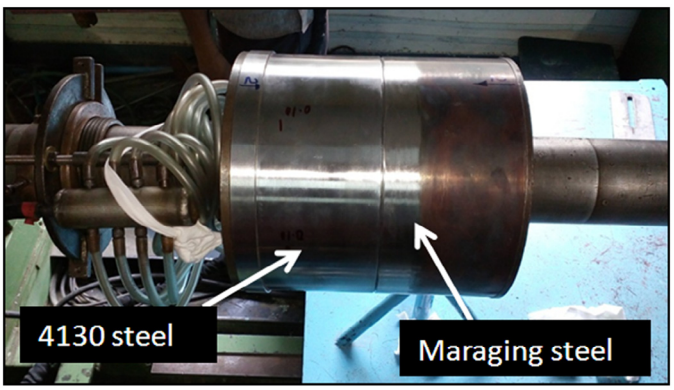

Fig. 1. Weld fixturing setup for both TIG and laser beam welding processes.

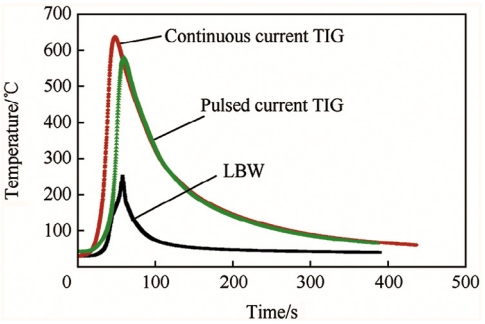

Fig. 2. Variation of peak temperatures in ICHAZ of AISI 4130 steel side during various welding processes.

2.5. Optical metallography and fractography

The weld joints were sectioned, mounted and mechanically polished as per laid down standard metallographic procedures. The fully polished metallographic specimens were then etched selectively by applying a 2% natal solution on AISI 4130 steel side and modified fry's reagent on weld zone as well as on HAZ of maraging steel side. The so etched various zones of weldment were studied under optical metallurgical microscope of OLYMPUS make. The fractured surfaces of tensile test specimen were examined under scanning electron microscope (ZEISS make) with an aim to capture the mode of failure.

3. Results and discussion

3.1. Visual examination of weld joints

The dissimilar steel weld joints are visually examined and it is observed that the laser beam welds have very less bead geometry as compared to that of both continuous and pulsed TIG welds. The extent of darkening in HAZ of dissimilar weld joints also was very much minimal in case of laser beam welds as compared to TIG welds. This could be due to the fact that the laser beam welding process imposes high power density and extremely low welding heat input compared to those of TIG welding process. All the welds are found to be defect-free as investigated through X-ray radiography and dye-penetrant tests.

3.2. Peak temperature profiles in ICHAZ

The peak temperatures measured during welding time at the locations adjacent to the weld in ICHAZ of AISI 4130 steel are presented in Fig. 2. The slope of the plot during heating is found to be lower than that of post weld cooling time. The laser beam

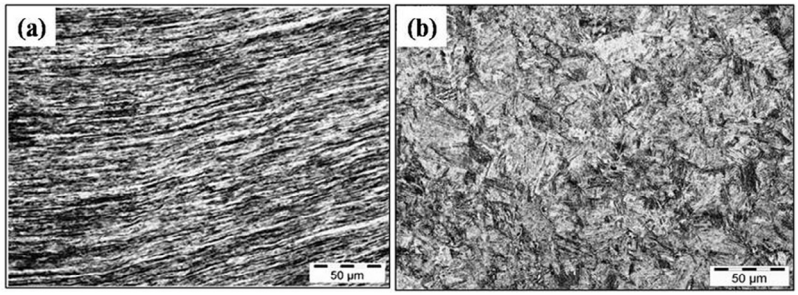

Fig. 3. Microstructures of parent materials. (a) Maraging steel; (b) AISI 4130 steel.

welds have resulted in lowest peak temperature in ICHAZ as compared to that of both continuous and pulsed TIG welds.

3.3. Optical microstructures

The optical microstructures of parent materials i.e., maraging steel in flow formed condition is shown in Fig. 3(a) and that of AISI 4130 steel in hardened and tempered condition is shown in Fig. 3(b). Very fine lath martensite features stretched along the flow forming lines are observed in the microstructure of maraging steel while the microstructures of AISI 4130 steel presents a tempered martensite phase.

The dissimilar steel weldment can be broadly categorized into four number of zones, i.e., fusion zone, HAZ of maraging steel, HAZ of AISI 4130 steel and unaffected parent material zones of both the dissimilar steels.

The microstructures of different zones of HAZ on maraging steel side of dissimilar steel weld made by continuous current TIG welding process are shown in Fig. 4. The HAZ on maraging steel side is made of three zones. The zone-A (Fig. 4(a)) is called as dark band zone because it attains dark color after etching. This zone (which experiences peak temperatures approximately 590 °C to 730 °C during welding) depicts two phase microstructure, wherein pools of reverted austenite are encircled by low carbon iron–nickel martensite. In the zone-B (Fig. 4(b)), parent metal (maraging steel) undergoes temperatures high enough to transform to austenite and upon cooling the martensite is formed. The zone-C (Fig. 4(c)) lies very next to fusion zone and the parent metal experiences austenite transformation and associated grain growth. Upon cooling, the austenite transforms to Fe–Ni martensite but inherits prior

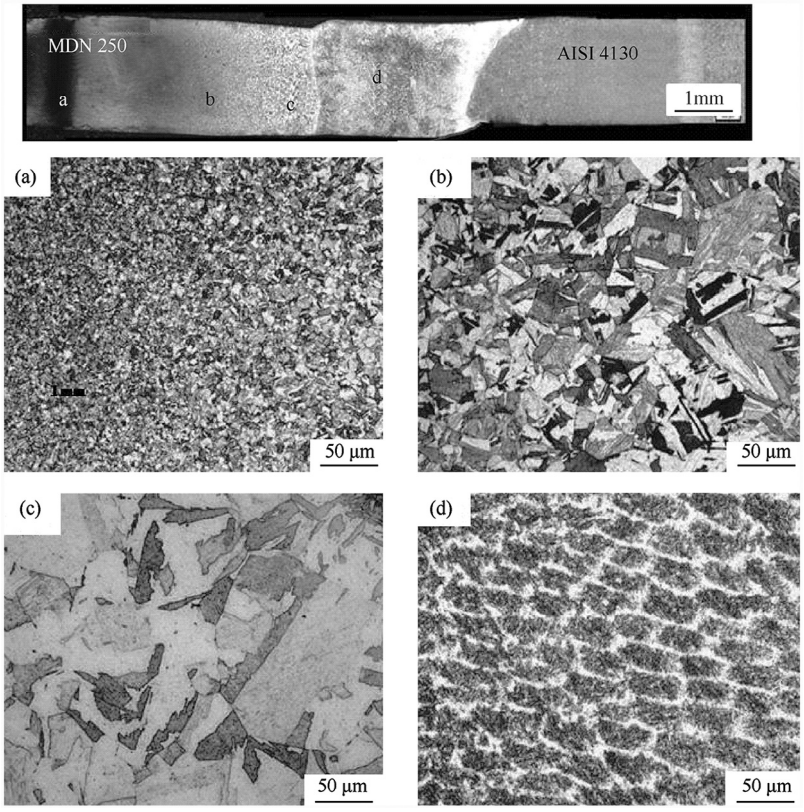

Fig. 4. The microstructures of different zones of HAZ on maraging steel side of dissimilar steel weld made by continuous current TIG welding process [8] (a) dark band zone, (b) fine grained HAZ, (c) coarse grained HAZ, and (d) fusion zone.

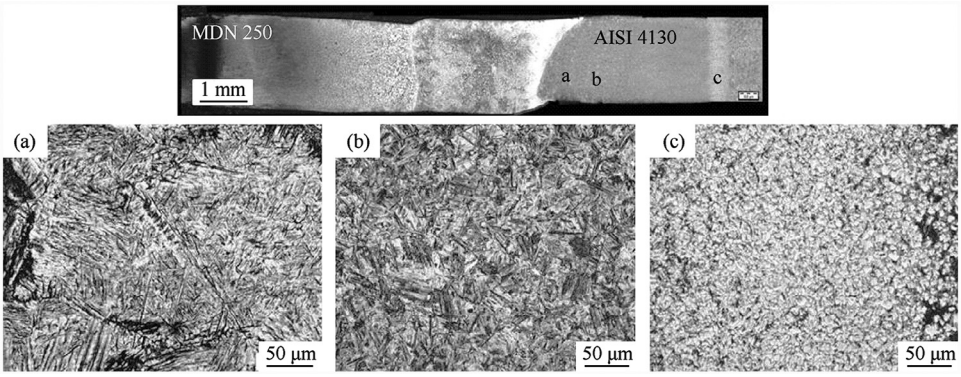

Fig. 5. The microstructures of different zones of HAZ of AISI 4130 steel of weld joint made with continuous current TIG welding process. (a) Coarse grained HAZ, (b) fine grained HAZ, and (c) inter critical HAZ [8].

austenite coarser grain size. The fusion zone ((Fig. 4(d)) reveals honey comb/cellular grain structure which is typical resultant of solidification process.

The microstructures of different zones of HAZ of AISI 4130 steel of weld joint made with continuous current TIG welding process are shown in Fig. 5. Largely the HAZ of AISI 4130 steel comprises of coarse grained (CG) HAZ, fine grained (FG) HAZ and inter-critical(IC) HAZ.

The CGHAZ (Fig. 5(a)) lies closest to fusion zone and experiences temperatures high enough to cause austenitic transformation and grain growth. When the zone is suddenly cooled, prior austenite grain size leads to coarser martensite phase formation in CGHAZ. In the FGHAZ (shown in Fig. 5(b)) the peak temperature near about AC_3 is reached, so the cooling causes finer grain size.

Microstructures of dissimilar steel weldments of different zones of laser beam weld joint toward maraging steel are shown in Fig. 6. The metallurgical changes in all these zones are as same as those of TIG welds however due to the very low heat input during laser beam welding process, the width of each zone is very minimal and almost negligible in case of dark band zone in HAZ of maraging steel. Very fine grain size is observed compared to that of the TIG welds across all the different zones (FGHAZ, CGHAZ and fusion zone).

The microstructures of different zones of HAZ toward AISI 4130 steel side of dissimilar steel weld produced through laser

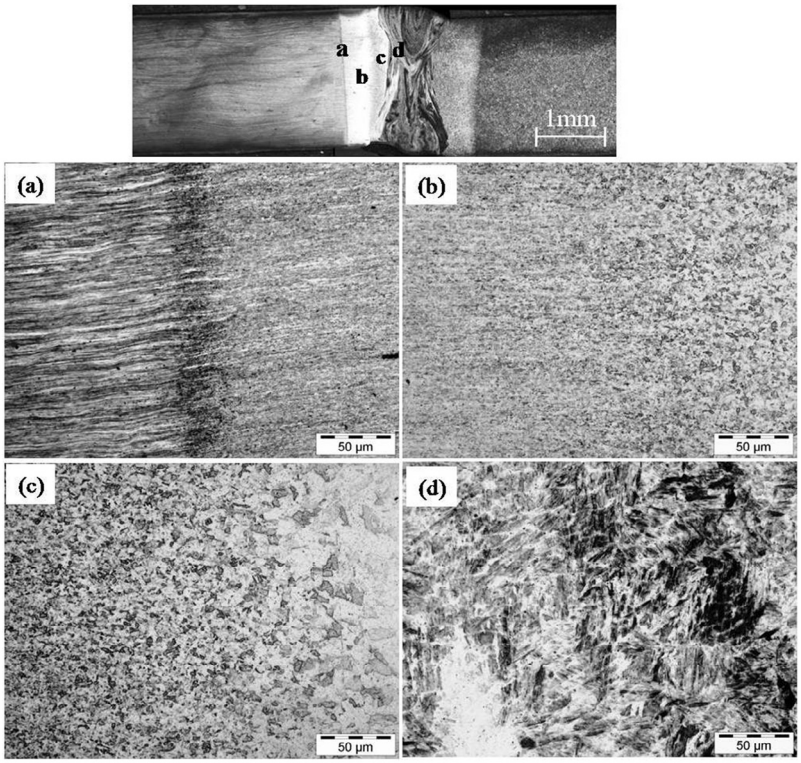

Fig. 6. The microstructures of different zones of HAZ toward maraging steel side of dissimilar steel weld produced through laser beam welding process. (a) Dark band region, (b) fine grained HAZ, (c) coarse grained HAZ, and (d) fusion zone.

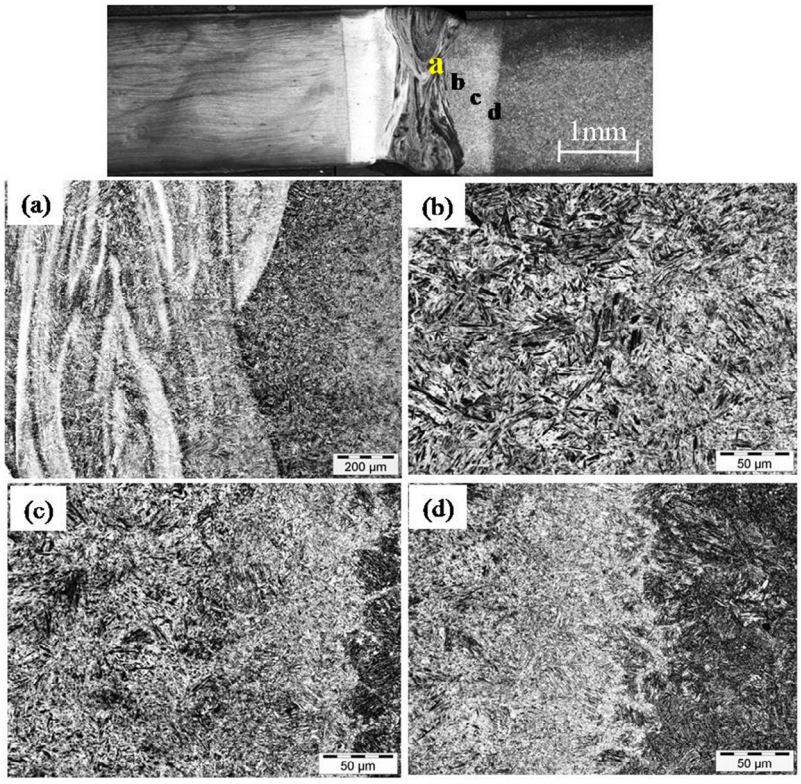

Fig. 7. The microstructures of different zones of HAZ toward AISI 4130 steel side of dissimilar steel weld produced through laser beam welding process. (a) Fusion zone, (b) Coarse grained HAZ, (c) Fine grained HAZ, and (d) ICHAZ.

beam welding process are shown in Fig. 7. The grain size in the CGHAZ and FGHAZ of laser beam welds is less than that of the TIG welds which could be due to the very low heat input and faster cooling rates experienced by these regions during weld cooling stage. The width of ICHAZ of laser beam weld is also found to be very less as compared to that of TIG welds.

The high magnification microstructures of ICHAZ corresponding to TIG welds (both continuous and pulsed current)

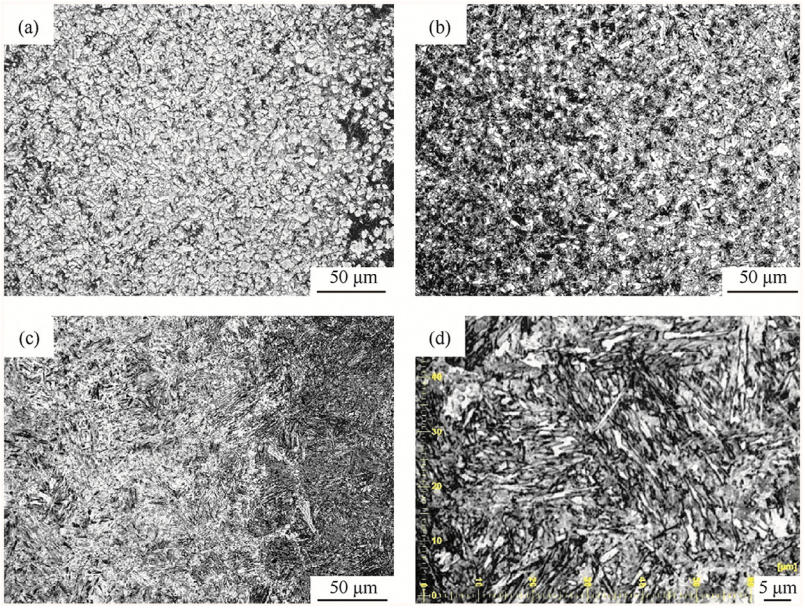

Fig. 8. The microstructures of ICHAZ in AISI 4130 steel side. (a) Continuous current TIG weld, (b) pulsed current TIG weld, (c) laser beam weld, and (d) laser beam weld at high magnification.

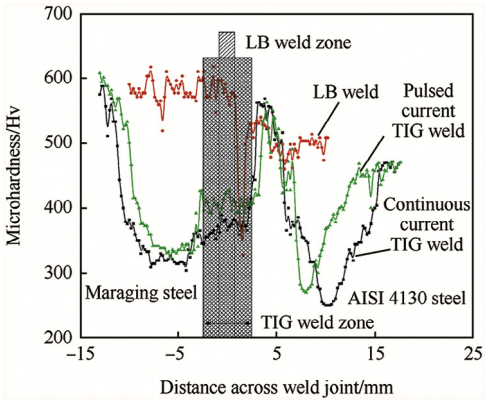

Fig. 9. A relative microhardness profile across the weldment at mid thickness of dissimilar steel weld produced through TIG and laser beam welding processes.

and laser beam weld are depicted in Fig. 8. One can easily observe from these microstructures that more amount of ferrite is present in the matrix of the weld joints made by continuous current TIG as compared to that of pulsed current TIG welding. It could be due to the fact that these zones undergo peak temperatures in the range of ~650 °C as measured and shown in Fig. 2**.** The amount of ferrite that is present in ICHAZ of laser beam weld is noticed to be very less than that is present in case of both the TIG welds. This could be because of the fact that the prevailing temperature in ICHAZ of laser beam weld is recorded to be around 250 °C that too for a very short duration as compared to TIG welds.

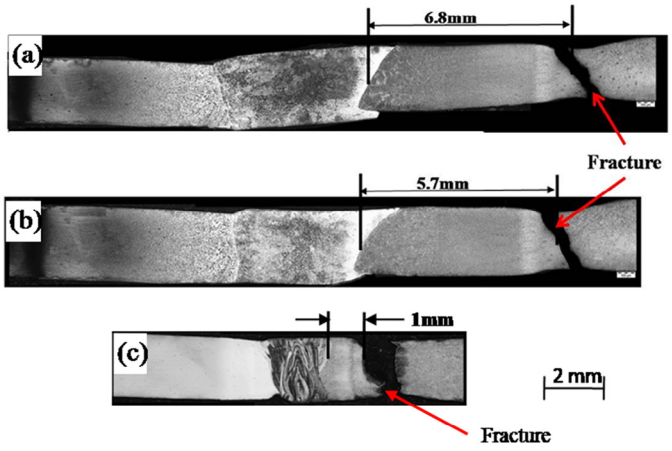

Fig. 10. Macro structures of fractured tensile test samples of dissimilar steel welds. (a) Continuous current TIG weld, (b) pulsed current TIG weld, and (c) fiber laser beam weld.

3.4. Microhardness profile across weldment

A relative microhardness profile across the weldment at mid thickness of dissimilar steel TIG and laser beam welds is shown in Fig. 9. In general, the microhardness of the fusion zone is measured to lesser as compared to the remaining all zones of weldment in case of all the three types of weld joints. The presence of very low carbon iron–nickel BCC martensite may be a reason for the lower hardness in fusion zone. The hardness of heat affected zones of both maraging steel and AISI 4130 steel is noticed to be lesser as compared to their respective hardness of parent materials. The CGHAZ (closest to fusion line) of maraging steel reported the hardness lower than the unaffected flow formed and aged parent material. This could be due to the fact that during weld thermal cycle, this zone of HAZ experiences temperatures beyond the solutionizing temperature dissolving all the strengthening precipitates. A local reduction of hardness in dark band zone away from fusion zone in HAZ of maraging steel is because of the presence of dual phase microstructure comprising of reverted austenite pools in the matrix of BCC martensite [1].

A clearly noticeable increase in the hardness as compared to fusion zone is reported in CGHAZ (very next to fusion line) of AISI 4130 steel. This CGHAZ of AISI 4130 steel goes through the peak temperatures above AC_3 line and upon sudden cooling during weld cooling stage, a hard martensite phase is formed similar to oil quenching heat treatment of carbon steels. However, the ICHAZ zone away from the fusion zone under goes relatively lower temperatures closer to AC_1, exhibited low hardness due to the presence of low temperature transformation phases surrounded by martensite. A similar finding was reported in research works by Nascimento and Voorwald [5]. However, the laser beam welds have not resulted in the reduction of the hardness in HAZ of maraging steel. This could be the fact that the heat input is much less during laser beam welding process.

The location and width of soft zone in HAZ of AISI 4130 steel of dissimilar steel welds produced with different welding processes are presented in Table 4. The soft zone in HAZ of AISI 4130 steel may be categorized by two considerations. One consideration is that any zone measured with hardness less than 400 Hv can be treated as soft zone. Second consideration is the location of least hardness from the fusion line. The fiber laser beam weld joints have demonstrated lowest width of soft zone and location of soft zone is close to the fusion line as compared to the TIG weldments. The degree of softening is minimum in low heat input welding process. This is due to the exposure of material to high temperatures for shorter duration, which led to absence of transformation to soft high temperature products.

Table 4
Softening tendencies in HAZ of AISI 4130 steel.

Type of welding process/ technique	Distance of soft zone from the fusion line/mm	Width of soft zone/mm	Minimum hardness in HAZ/Hv	Maximum hardness in HAZ/Hv
Continuous current TIG weld	7.0	10	259	556
Pulsed current TIG weld	5.0	4.5	271	548
Laser beam weld	1.0	0.25	350	545

Table 5
Tensile properties of different dissimilar steel welds.

	UTS/MPa	0.2% YS/MPa	El./%	Weld joint efficiency based on UTS	Distance of fracture location from fusion zone on AISI 4130 steel side/mm
Continuous current TIG weld	960	826	3.8	62.74	4.16
Pulsed current TIG weld	995	885	3.4	65.03	4.90
Fiber laser beam Weld	1494	1215	2.2	97.6	1.0

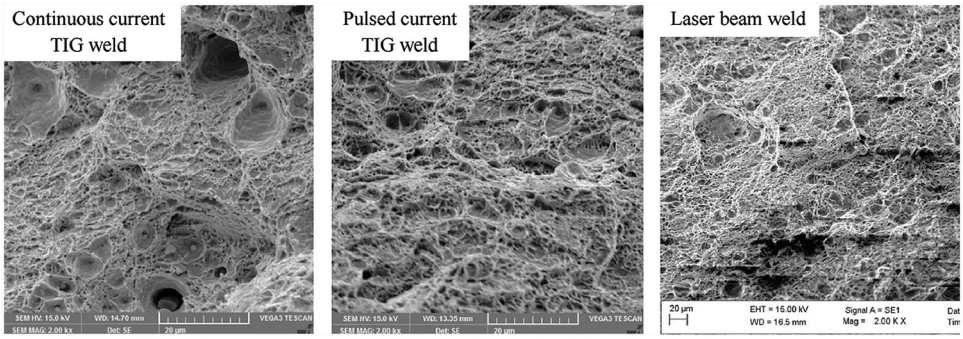

Fig. 11. Fractographs of fractured surfaces of tensile test samples of dissimilar steel welds made by different welding processes.

This shows that the laser beam welding process has induced minimum heat input as compared to TIG welding process irrespective of welding technique (continuous current mode or pulsed current mode) employed.

3.5. Tensile properties

The transverse tensile properties of dissimilar steel welds produced with different welding processes and technique are shown in Table 5. The macrostructures of fractured tensile test samples that clearly reveal the location of fracture in ICHAZ of AISI 4130 steel are shown in Fig. 10. The fracture of tensile test specimen is noticed to be located in the same zone of lowest hardness reported in the microhardness survey as mentioned in Fig. 9.

The tensile properties of laser beam weld joints were superior to those of both the TIG weld joints. The location of fracture in case of laser beam weld joints was relatively closer to the fusion line when compared to that of TIG welds, which is in tune with the microhardness profile shown in Fig. 9. This could be due to the fact that the welding heat input was drastically reduced during laser beam welding process. Use of fiber laser beam welding has enhanced the weld joint efficiency in terms of ultimate tensile strength from 62 to 97.6%.

3.6. Fractography

The captured fractographs by scanning electron microscopy conducted on fractured surfaces of tensile test samples of all dissimilar steel welds are shown in Fig. 11. It is clearly evident from the fractographs that the fracture surfaces of welds made with continuous TIG welding process show deeper and wider dimples as compared to that of pulsed TIG welds and laser beam welds. The fracture surfaces of laser beam welds depict finer and shallow dimples.

4. Conclusions

An effective comparative study has been conducted on the microstructural and mechanical behavior of dissimilar steel welds produced by TIG welding and laser beam welding process. The significant outcome of this study is mentioned below.

1) Laser beam weld joints have shown higher weld joint efficiencies as compared to both continuous current and pulsed current TIG weld joints.
2) The rapid heating and cooling experienced by the HAZ of AISI 4130 steel during fiber laser beam welding process has resulted in reduced width of HAZ in AISI 4130 steel.
3) Use of laser beam welding process has improved the joint efficiency from 62% to 97% in terms of ultimate tensile strength.

Acknowledgment

The authors are highly grateful to the Director, Defence Research and Development Laboratory (DRDL), Hyderabad, for according permission to publish this work and also to the Director, National Institute of Technology (NIT), Warangal for support extended in conducting this work.

References

[1] Lang FH, Kenyon N. Welding of maraging steels. WRC Bull 1959;1–41.
[2] Olson DL, Siewert TA, Liu S. ASM handbook. Properties and selection: irons, steels, and high-performance alloys, vol. 1. Materials Park (OH): ASM International; 1990.
[3] Hamada M. Control of strength and toughness at the heat affected zone. Weld Int 2003;17(4):265–70.
[4] Lee IK, Chien YC. A study on microstructure and mechanical properties of thick welded joints of a Cr-Mo steel. Met Sci Heat Treat 2015;57(3):175–80.

[5] Nascimento MP, Voorwald HJ. Considerations on corrosion and weld repair effects on the fatigue strength of a steel structure to the flight safety. Int J Fatigue 2010;32:1200–9.
[6] Yan HQ, Wu KM, Wang HH, Li L, Yin YQ, Wu NC. Effect of fast cooling on microstructure and toughness of heat affected zone in high strength offshore steel. Sci Technol Weld Joi 2014;20(2):145–54.
[7] Dong H, Hao X, Deng D. Effect of welding heat input on microstructure and mechanical properties of HSLA steel joint. J Metallograph Microstruct Anal 2014;3:138–46.
[8] Joshi JR, P. M, A. K, G. MR, K. RK. Influence of welding techniques on heat affected zone softening of dissimilar metal maraging steel and high strength low alloy steel gas tungsten arc weldments. T Indian I Metals 2016;doi:10.1007/s12666-016-0861-4.
[9] Huang CC, Pan YC, Chuang TH. Effects of post weld heat treatments on the residual stress and mechanical properties of electron beam welded SAE 4130 steel plates. J Mater Eng Perform 1997;6:61–8.
[10] Chang Y, Wang C. Effect of post weld heat treatments on the fatigue crack growth rate of electron beam welded AISI 4130 steel. Metall Mater Trans A 1996;27A:3162–9.
[11] Souza Neto F, Neves D, Silva OMM, Lima MSF, Abdalla AJ. An analysis of the mechanical behaviour of AISI 4130 steel after TIG and Laser welding process. Procedia Eng 2015;114:181–8.
[12] Quintino L, Costa A, Miranda R, Yapp D, Kumar V, Knong CJ. Welding with high power fiber lasers – a preliminary study. Mater Des 2007;28(4):1231–7.